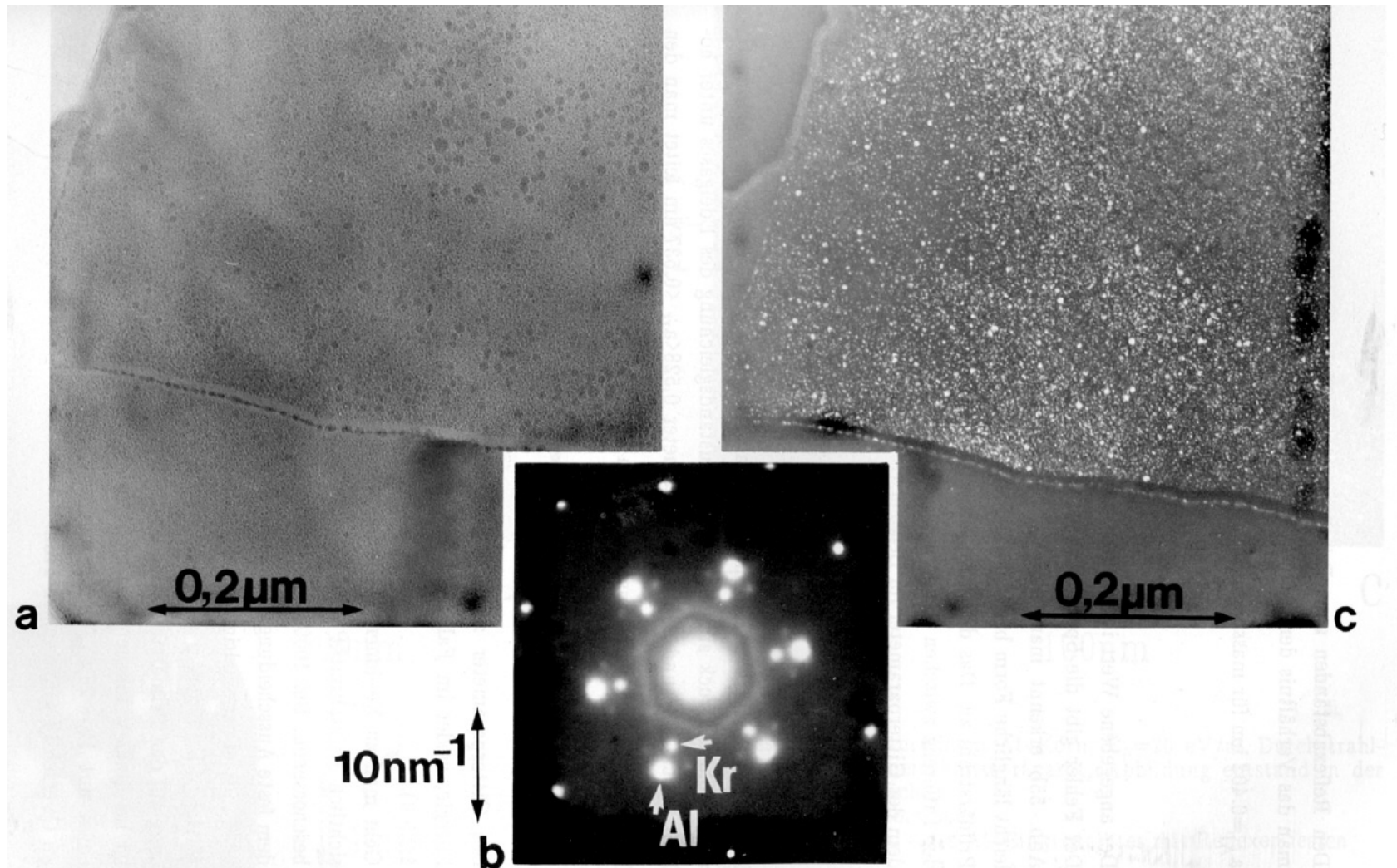


Solid Kr Precipitates Formed in Ion Beam Assisted Deposition of Al

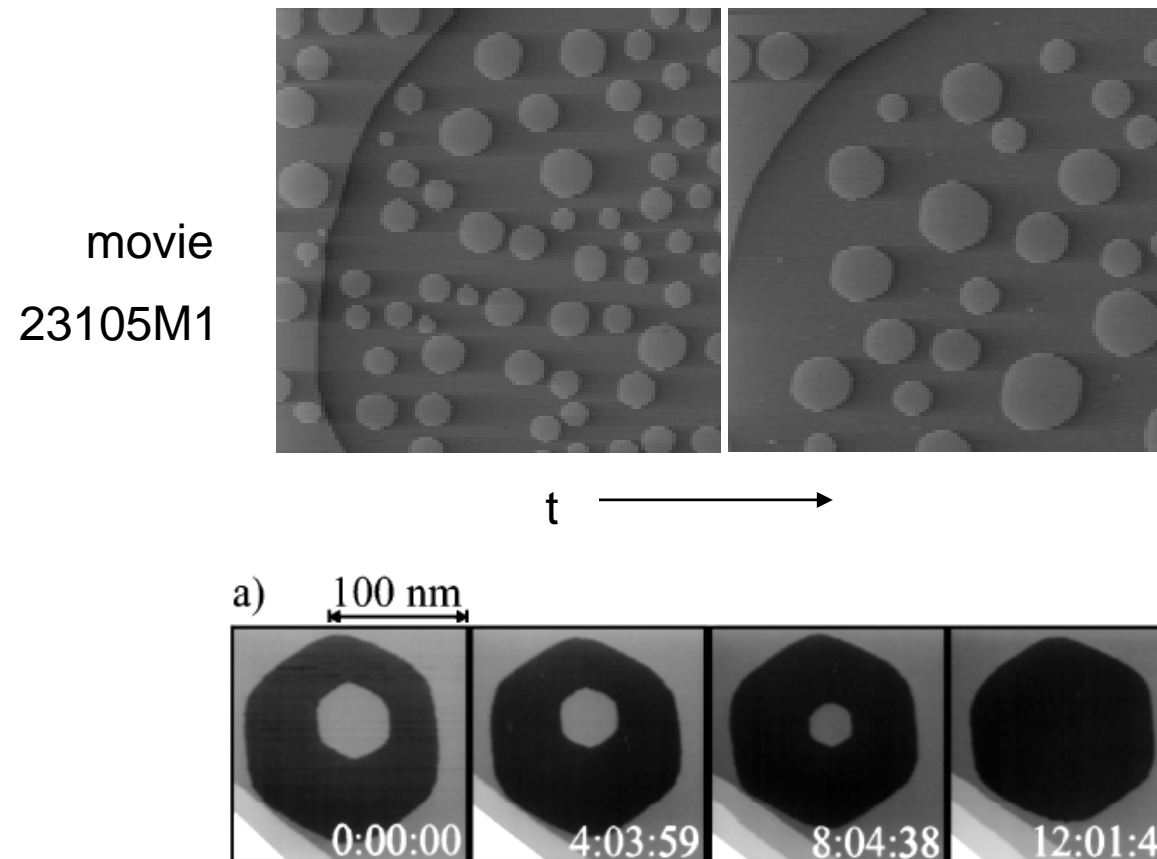


Kr-Ausscheidungen in Al-Körnern und an einer Korngrenze
 $E_n=100 \text{ eV}/\text{at}$, Durchstrahlrichtung $\langle 111 \rangle$, zur Oberfläche rückge-
dünnte Probe

a) Hellfeld, 0,8 μm Überfokus
b) $\langle 111 \rangle$ -SAD-Bild eines Al-Einkristallites mit Reflexen festen
Kryptons

c) Dunkelfeldbild der Probenstelle aus a), $g_{\text{Kr}}=\langle 2\bar{2}0 \rangle$ Fig. 4.3

Ostwald Ripening and Island Decay on Ag(111)



K. Morgenstern et al. PRL 80 (1998) 556

Fig. 4.4

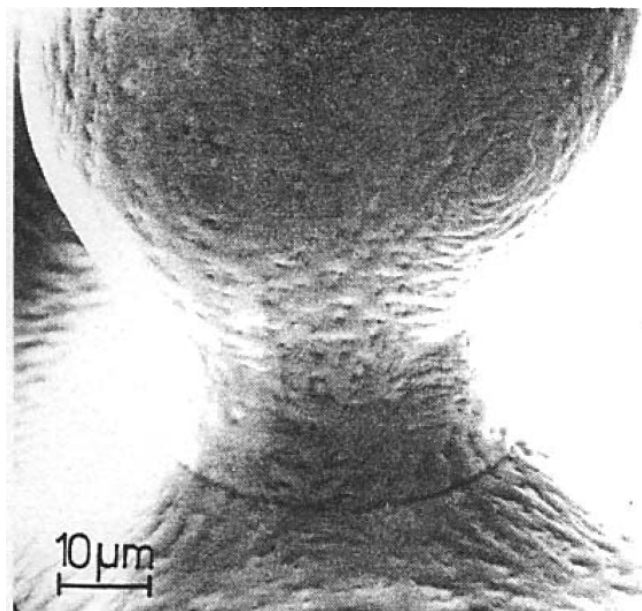


Fig. 3. Scanning electron micrograph of a ball sintered onto a single crystal plate.

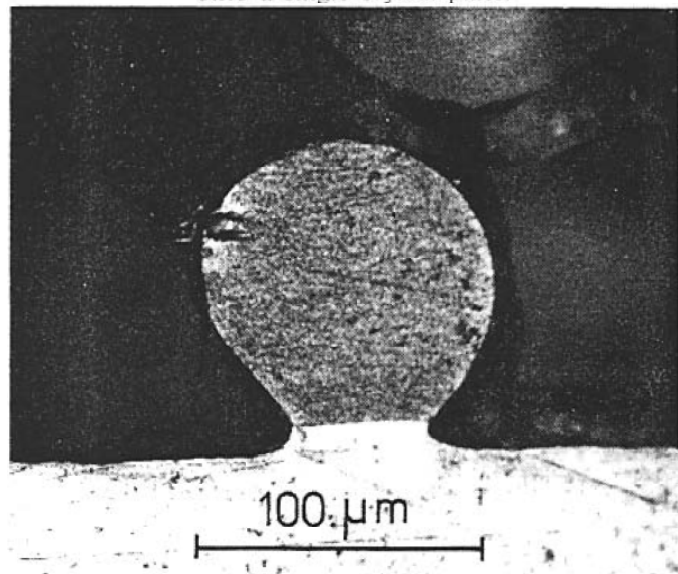


Fig. 5. Light micrograph of a cross sectioned and chemically etched, annealed specimen demonstrating the location of the grain boundary between ball and plate.

Sintering of Balls and Wires

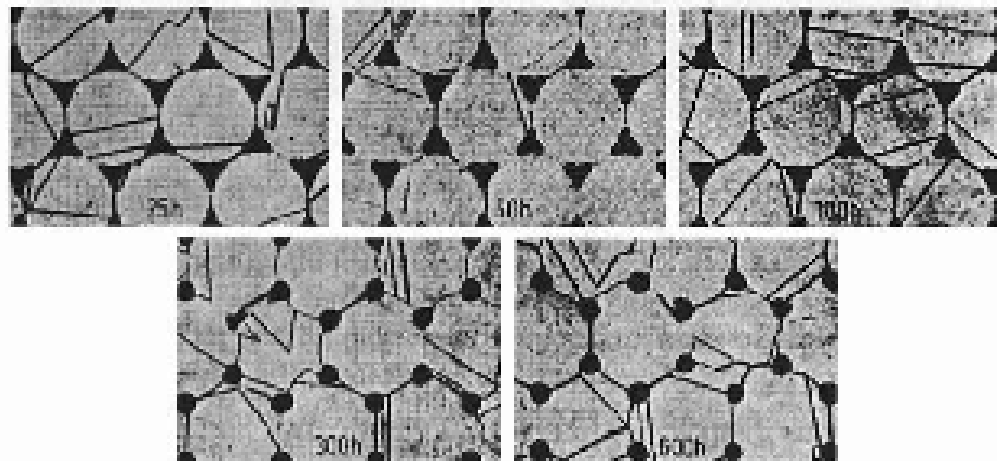


Fig. 8.19. Section through a bundle of copper wires (diameter 30 μm) after annealing at 900°C for the times given. The wires grow together at necks and the pores become rounded off.

Fig. 4.5

G. Herrmann, H. Gleiter, G. Bäro, Act. Metall. 24, (1976) 353

Coarsening During Ion Erosion

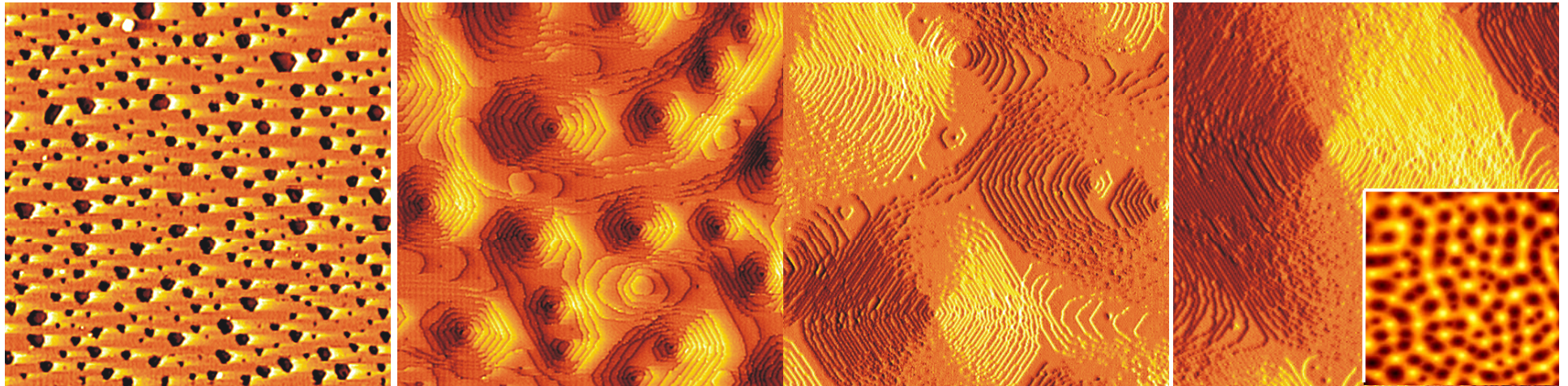


FIG. 1. STM topographs after erosion of (a) 0.26 ML, (b) 6.2 ML, (c) 66 ML, and (d) 333 ML at 500 K
Topograph width 810 Å for (a)–(d)

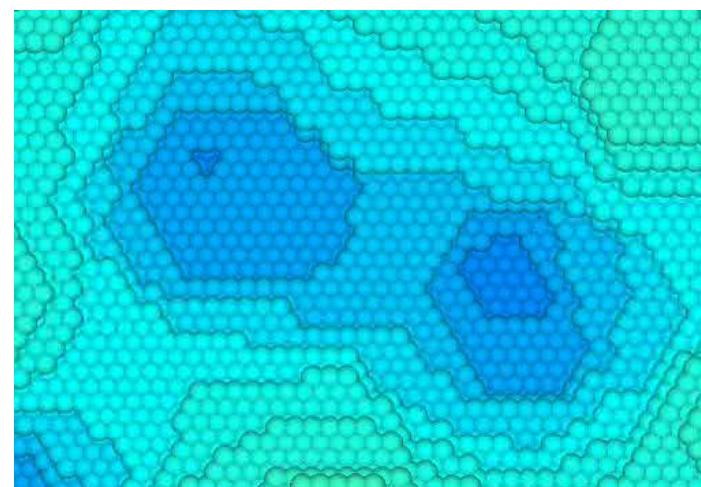


Fig. 4.6

T. Michely et al. PRL 86 (2001) 2589

KMC

Grain Grooving and Grain Growth

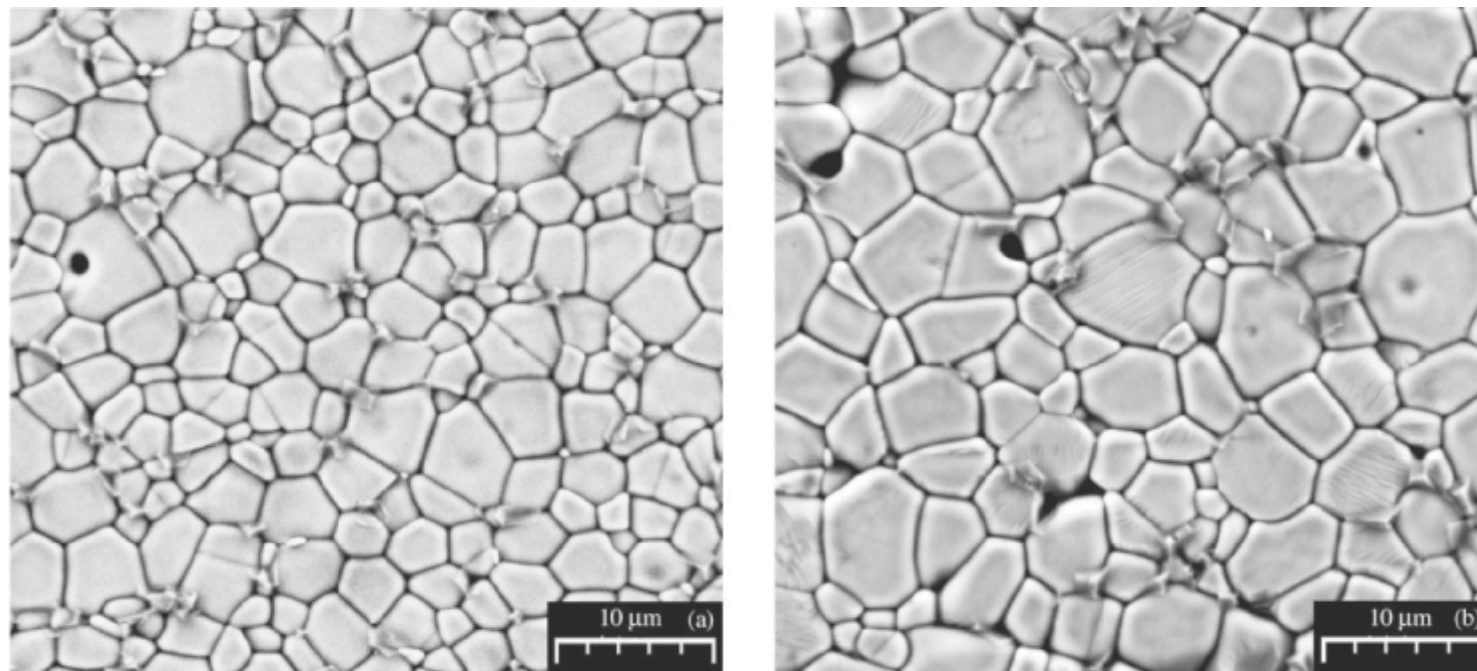


Figure 4. SEM micrographs of the SMNb0.2% composition sintered at 1300 °C for: (a) 1 h; (b) 4 h.

Fig. 4.7